THE JOURNAL OF PHYSICAL CHEMISTRY C

Article

pubs.acs.org/JPCC

Theoretical Study on Noncovalent Interactions in the Carbon Nanotube−Formic Acid Dimer System

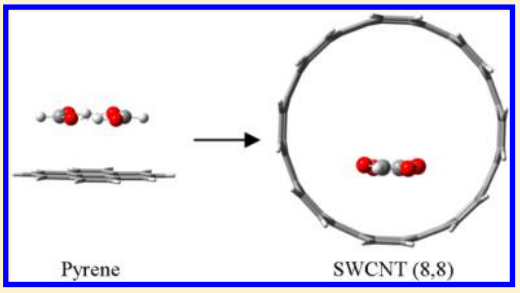
Piotr Okrasiński,*[,†] Zdzisław Latajka,*[,†] and Christof Hättig[‡]

[†]Faculty of Chemistry, University of Wrocław, F. Joliot-Curie 14, 50-383 Wrocław, Poland

[‡]Lehrstuhl für Theoretische Chemie, Ruhr-Universität Bochum, D-44780 Bochum, Germany

Supporting Information

ABSTRACT: The noncovalent interaction of the formic acid dimer (FAD) with pyrene and single-walled carbon nanotubes (SWCNTs) is studied using both density functional theory with an empirical dispersion correction as well spin-component-scaled and F12 variants of second-order Møller−Plesset perturbation theory. For the FAD−pyrene model system, it is shown that the dispersion-corrected DFT methods provide similar accurate results for the noncovalent interaction of carboxylic acid dimers with large conjugated π-systems such as MP2 and SCS-MP2. The binding energy of FAD in SWCNTs is found to be sensitive to the radius of the nanotube. It amounts to ca. 22 kcal/mol in the armchair (6,6) SWCNT and decreases with increasing tube radius. In the armchair (8,8) SWCNT, the binding energy is already 25% smaller. To facilitate an experimental identification of FAD inside SWCNTs, we report results for the shifts of the vibrational frequency, where we could identify intense C−O, C═O and O−H stretch modes as promising infrared signatures for an experimental detection of such complexes.



INTRODUCTION

Carbon nanotubes (CNTs) play an important role in materials chemistry and are the subject of many experimental and theoretical studies.[1−5] Open-ended single-walled carbon nanotubes (SWCNTs) are considered in many studies as a model system in nanoconfined chemistry. Because of their special structure (the tubular morphology), CNTs might be considered as "nanoreactors" for chemical reactions.[6]

The confinement of simple molecules inside the SWCNTs is widely studied because they exhibit in this environment a different behavior than on the exterior of SWCNTs.[6−9] There are many theoretical studies on the encapsulation of water particles inside nanotubes, for example, analysis of the interactions,[10] density,[11] or water and proton transfer through the SWCNT (as model for biological channels).[12] Furthermore, endohedral filling allows us to preserve unique quasi-1D electronic properties of CNTs.[13]

The cyclic formic acid dimer (FAD) is one of the simplest systems with a double hydrogen bond and the textbook example for complexes with proton transfer, which is a ubiquitous reaction in several chemical and biological systems, and for the structure and reactivity of certain proteins and double-stranded DNA.[14−18] The possible double proton transfer is the main reason for widespread interest in experimental and theoretical studies of FAD and other simple carboxylic acids.[19−23]

In the present study, we have considered only endohedral encapsulation of FAD inside SWCNTs. This decision was driven by the size of the system and great computational cost. Encapsulation of different molecules or small intermolecular systems inside CNTs has been less studied, but according to Pan and Bao,[6] such confinement can provide novel environment for catalytic reactions.

In our study, we first analyzed the noncovalent interaction between the FAD and pyrene, which is used as a simple model for a CNT wall. This allowed the use of more sophisticated and computationally demanding calculations with explicitly correlated MP2 theory to validate and justify the use of dispersion-corrected DFT methods for the description of such systems. We then calculated the equilibrium structures and binding energies for FAD in an armchair (6,6) SWCNT as an example for a smaller nanotube and in an armchair (8,8) SWCNT as an example for a larger one. To allow for an easier comparison of our theoretical predictions with future experimental results, we evaluated in addition to the structure and binding energies vibrational frequencies and infrared intensities.

COMPUTATIONAL DETAILS

All calculations were carried out with the TURBOMOLE program package[24,25] and used resolution of identity (RI) approaches at the DFT[26] and the conventional[27,28] and explicitly correlated MP2 level.[29] All basis sets were taken from the TURBOMOLE library, and for the RI approximation the one-electron basis sets were combined with the corresponding optimized auxiliary basis sets from refs 26 and 30−32.

For the FAD on pyrene, the geometry optimization was carried out at the PBE-D3, PBE0-D3, and B3LYP-D3 levels

Received: December 2, 2013
Revised: February 3, 2014
Published: February 4, 2014

Downloaded via BOCHUM LIBRARIES on January 16, 2019 at 10:17:38 (UTC).
See https://pubs.acs.org/sharingguidelines for options on how to legitimately share published articles.

© 2014 American Chemical Society

dx.doi.org/10.1021/jp411801h | J. Phys. Chem. C 2014, 118, 4483−4488

with the TZVP basis set,[33] and for the SWCNT-based complexes it was carried out at the PBE-D3 level with SVP[34] and TZVP basis sets.

The interactions between the FAD and pyrene were also studied with MP2 and the hierarchy of augmented correlation-consistent basis sets[35] aug-cc-pVXZ with X = D, T, Q, and MP2-F12 using the cc-pVDZ-F12 and cc-pVTZ-F12 basis sets,[36] always at the DFT geometry (B3LYP-D3/def2-TZVP). All interaction energies presented in this work are corrected for the basis set superposition error (BSSE) using the standard counterpoise correction of Boys and Bernardi.[37]

Density functional calculations were carried out with generalized gradient and hybrid and double hybrid functionals and included the empirical D3 dispersion correction.[38] Wave-function-based calculations were carried for the van der Waals complexes of the formic acid monomer and its dimer with pyrene, which is used as a simple model for an SWCNT wall. Second-order Møller−Plesset perturbation theory (MP2) was applied for this purpose with and without spin-component scaling to test and improve its stability.

In the spin-component scaled (SCS)[39,40] variant of MP2, the second-order correction from double excitations of electron pairs with parallel- and antiparallel-spin are scaled with separate optimized factors. It is described by the following equation:

$$E^{\mathrm{corr}}(\mathrm{SCS\text{-}MP2}) = p_{\mathrm{S}}E_{\uparrow\downarrow} + p_{\mathrm{T}}E_{\uparrow\uparrow+\downarrow\downarrow}$$

where we used the default scaling parameters $p_S = 6/5$ and $p_T = 1/3$.

In MP2-F12,[41] the conventional excitations into products of unoccupied one-electron orbitals are augmented by excitations of electron pairs into explicitly correlated pair functions, which are constructed as $\hat{Q}_{12}f_{12}\varphi_i\varphi_j$, where $f_{12} = 1 - \exp(-\gamma r_{12})$. The exponent γ was in all calculations set to the value optimized for the employed one-electron basis set, which was combined with the optimized auxiliary basis sets from ref 42. No extrapolation techniques have been used in the F12 calculations.

In addition, we used estimated complete basis set (CBS) limits,[43] which were determined by an extrapolation based on the dependence of the (non-F12) MP2 correlation energy on the cardinal numbers X and $Y = X - 1$ as:

$$E_{\mathrm{corr}}(\infty) \approx \frac{E_{\mathrm{corr}}(X)\cdot X^3 - E_{\mathrm{corr}}(Y)\cdot Y^3}{X^3 - Y^3}$$

This approach allowed us to obtain accurate results close to the basis set limit already with a small cardinal number; that is, extrapolated DZ/TZ results are usually slightly more accurate than those obtained with the QZ basis set without extrapolation.

RESULTS AND DISCUSSION

Our study was focused mainly on the influence of SWCNTs on the structure and the properties of the FAD. First, we analyzed the geometry changes of FAD relative to the gas-phase values in the studied systems, that is, interacting with pyrene and the two armchair CNTs with different diameters (structures are presented in Figure 1). The results of geometry optimizations revealed that the internal geometry of the FAD changes little upon interaction with pyrene or the SWCNT wall. The lengths of C−O and C═O bonds stay unchanged (e.g., for PBE-D3/def2TZVP, the values are 1.31 and 1.23 Å, respectively) and are very similar to those observed experimentally in gas electron diffraction, 1.323 and 1.220 Å, respectively.[44] It is, however,

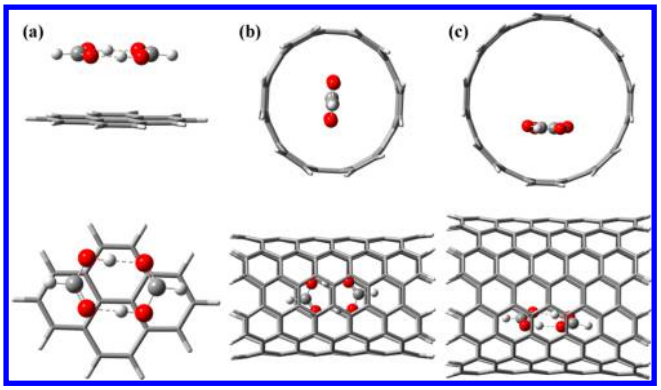


Figure 1. Structures of analyzed systems: (a) FAD on pyrene, (b) FAD inside the (6,6) SWCNT 15 Å, and (c) FAD inside the (8,8) SWCNT 15 Å.

found that the length of the hydrogen bridge (O···H−O) depends on the exchange-correlation functional and changes from 2.59 for the PBE-D3 functional to 2.66 Å for the hybrid functional B3LYP-D3. The latter results are smaller than those obtained in the experiment, in which the length of the hydrogen bridge in the FAD was determined to be 2.703 Å.[44] The deviation is, however, in particular for B3LYP-D3, small and might be partially due to the fact that we compare a calculated geometrical structure at the minimum of the potential energy surface (r_e structure) with an experimental, vibrationally averaged structure. According to our knowledge, there is still a lack of published results for the FAD geometry from high-level calculations, that is, CCSD(T), that could be used as additional benchmark.

A very useful method to characterize the H-bond interaction is the natural bond orbital (NBO) analysis.[45,46] Weinhold shows that the charge-transfer stabilization energy (ΔE_{CT}) due to transfer of electrons from the lone pair of proton acceptor to the antibonding orbital of X−H of proton donor is proportional to the hydrogen bond strength.[45] In Table 1 are presented values of charge-transfer stabilization energies for one of the O−H···O hydrogen bonds in the isolated FAD and FAD on pyrene. NBO analysis shows that the two lone pairs of the oxygen atom from carbonyl group have contributed to the O−H···O hydrogen bond. Moreover, the values of charge-transfer stabilization clearly show the stronger H-bond interaction when the FAD interacts with pyrene. In other words, the interaction with pyrene and probably also with SWCNT wall provides additional stabilization of hydrogen bond in FAD.

Table 1. Calculated Charge Transfer Stabilization Energy (ΔE_{CT}, in kcal/mol) for the O−H···O Hydrogen Bond of FAD

	ΔE_{CT}	
	FAD	FAD + pyrene
	B3LYP-D3/def2-TZVP	
$n_{O(lp1)} \rightarrow \sigma^*_{O-H}$	8.96	9.26
$n_{O(lp2)} \rightarrow \sigma^*_{O-H}$	21.69	22.78
	PBE-D3/def2-TZVP	
$n_{O(lp1)} \rightarrow \sigma^*_{O-H}$	9.49	9.58
$n_{O(lp2)} \rightarrow \sigma^*_{O-H}$	31.02	32.23
	PBE0-D3/def2-TZVP	
$n_{O(lp1)} \rightarrow \sigma^*_{O-H}$	10.32	10.52
$n_{O(lp2)} \rightarrow \sigma^*_{O-H}$	28.16	28.64

dx.doi.org/10.1021/jp411801h | J. Phys. Chem. C 2014, 118, 4483−4488

The results of the interactions between the FAD and pyrene are presented in Table 2. For the MP2 calculations, we also

Table 2. MP2 Interaction Energies of Formic Acid Dimer (FAD) with Pyrene[a]

method	E_{INT}	E_{EXT} (∞)
MP2/aug-cc-pVDZ	−8.83	
MP2/aug-cc-pVTZ	−9.43	−10.14
MP2/aug-cc-pVQZ	−9.98	−10.09
MP2-F12/cc-pVDZ-F12	−9.79	
MP2-F12/cc-pVTZ-F12	−10.03	
SCS-MP2/aug-cc-pVDZ	−6.60	
SCS-MP2/aug-cc-pVTZ	−7.12	−7.43
SCS-MP2/aug-cc-pVQZ	−7.29	−7.39
SCS-MP2-F12/cc-pVDZ-F12	−7.18	
SCS-MP2-F12/cc-pVTZ-F12	−7.38	

[a]Geometry optimized on B3LYP-D3/def2-TZVP level. E_{INT} is interaction energy without CBS limit correction; $E_{EXT}(\infty) = E_{MP2}(\infty) + E_{RHF}$ in highest basis set. All calculations were carried with CP correction to eliminate BSSE (values of energy in kilocalories per mole).

extrapolated the CBS limits. The results are, in particular for the TZ/QZ extrapolation, in very good agreement with the reference results obtained with explicitly correlated MP2-F12 in the F12 triple-ζ basis. The differences are very small. For MP2 with and without explicitly correlated F12 correction, it is −10.03 and −10.09 kcal/mol. However, MP2 is known to overestimate the dispersion interaction in π-stacked systems[47] and SCS-MP2 constitutes a significant improvement for the interaction between, for example, two π systems.[48,49] For SCS-MP2 the estimate for the basis set limit obtained from the TZ and QZ results is −7.39 kcal/mol, in perfect agreement with MP2-F12/cc-pVTZ-F12 value of −7.39 kcal/mol.

As can be seen from the results collected in Table 3, the values for the binding energy between FAD and pyrene obtained from the DFT calculations with the D3 dispersion correction in the valence triple-ζ basis are <1 kcal/mol smaller than those from SCS-MP2. For pyrene and the armchair (8,8) SWCNT, the SVP basis underestimates the interaction energy significantly. For the FAD inside the armchair (6,6) SWCNT, the differences between the double- and triple-ζ basis set results are smaller. In summary, the good agreement between the MP2 and the dispersion-corrected DFT results suggests that even the generalized-gradient functional with dispersion correction, PBE-D3, can be used to predict properties for extended systems such as the CNTs and is a good compromise between accuracy and computational costs.

Another important conclusion from the result in Table 3 is that the interaction of FAD with SWCNT inner walls is stronger than that with pyrene. This is related to the size and the curvature of SWCNTs that enclose the FAD dimer from several sides. In the armchair (6,6) SWCNT, the FAD dimer interacts with both faces equally strong with the SWCNT inner wall, and the large van der Waals contact surface leads to an attractive energy of ∼20 kcal/mol. This conclusion is confirmed by the result for the wider (8,8) armchair SWCNT, where the radius is too large for the FAD to have a close to optimal contact with both faces to the SWCNT inner wall. For this system, the binding energy is ca. 25% smaller than that for the (6,6) armchair SWCNT.

It is interesting to point out that detailed analysis of data presented in Table S1 (Supporting Information) shows only negligible changes in the HOMO−LUMO energy gaps of pyrene and SWCNT after inclusion of the FAD.

To facilitate a comparison of our theoretical predictions with experiment, we calculated in the next step of our study the vibrational frequencies for FAD in interaction with pyrene and two SWCNTs using analytical and numerical methods to obtain data for the influence of the interaction on the vibrational spectrum of FAD, which will by experimentally more easily accessible than its structure and binding energy. First of all, we calculated the vibrational frequencies for FAD in vacuum and compared them with the experimental data from ref 20 to determine scale factors for the frequency calculations on the interacting systems. The results are presented in Table 4, whereas the differences between the calculated and experimental frequencies are visualized in Figure 2. A good agreement is observed between the calculated and experimental frequencies for the isolated FAD. An exception is the asymmetrical O−H mode. Calculated values with the generalized gradient approximation (GGA) exchange-correlation PBE functional are underestimated by ca. 250 cm^{-1}. Similar discrepancy for the O−H stretching mode was also noted by Nadykto and coworkers for the FAD and other systems calculated with BLYP and PW91, which belong to the GGA functionals.[50] Moreover, many years ago for the HF dimer we observed similar results for the GGA functionals.[51] Nevertheless, for our consideration are important relative frequency changes due to the interaction with pyrene and SWCNTs but not absolute values of frequencies.

The numerical force constant calculation implemented in TURBOMOLE permits us to "freeze" some atoms to compute only the force constants and vibrational frequencies for the main interesting part of the system. This allows us to keep the computational costs tractable even for frequency calculations in such extended systems like CNTs, where we have over 100

Table 3. Interactions Energies of Formic Acid Dimer with Pyrene and Single-Walled Carbon Nanotubes Obtained in DFT-D3 Methods[a]

method	type	pyrene	(6,6) SWCNT	(8,8) SWCNT
PBE-D3/def2-SVP	GGA	−5.85	−20.78	−14.10
PBE-D3/def2-TZVP	GGA	−6.61	−20.79	−15.14
PBE0-D3/def2-TZVP	H	−6.78	−24.78	−15.71
B3LYP-D3/def2-TZVP	H	−7.04	−21.92	−17.00
B2PLYP-D3/def2-TZVP	DH	−6.25		
B2PLYP-D3/aug-cc-pVTZ	DH	−6.75		

[a]For pyrene, structures were optimized on the same level, and for calculations with SWCNT we used PBE-D3/def2-TZVP optimized structures and performed only single-point calculations (values of energy in kilocalories per mole).

dx.doi.org/10.1021/jp411801h | J. Phys. Chem. C 2014, 118, 4483−4488

Table 4. Calculated Vibrational Frequencies of Formic Acid Dimer Were Compared with Values Obtained in Different Experiments, Collected by Ito in Ref 20[a]

	wavenumbers (cm^{-1})		
type	exp (ref 20)	PBE-D3/def2-SVP	PBE-D3/def2-TZVP
twist	69.20	84.89	75.47
O−H−O ipb	165.00	184.72	178.38
γ(O−H−O) opb	168.47	205.18	193.04
O−O str.	194.00	243.47	222.23
O−H−O opb	242.00	298.44	273.49
O−H−O str.	269.00	346.51	314.18
O−C═O bend.	680.00	685.49	673.93
O−C═O bend.	698.00	734.84	719.89
δ(O−H) opb		1002.55	987.79
δ(O−H) opb	922.00	1013.05	995.70
δ(C−H) opb	1059.70	1093.57	1049.80
δ(C−H) opb	1050.00	1136.68	1098.77
C−O str.	1214.00	1278.96	1238.99
C−O str.	1230.20	1278.08	1240.47
H−C−O bend.	1364.00	1362.94	1351.47
H−C−O bend.	1374.80	1370.00	1356.87
C−O−H bend.	1454.00	1431.81	1428.35
C−O−H bend.	1415.00	1469.71	1459.82
C═O str.	1669.90	1644.76	1611.29
C═O str.	1746.00	1765.01	1710.18
sym. O−H str.		2564.63	2626.38
asym. O−H str.	3084.00	2759.61	2787.72
C−H str.	2938.50	2980.71	2980.29
C−H str.	2948.90	2982.83	2983.45
scaling factor		1.00347 ± 0.0123	1.01198 ± 0.0104
mean deviation (MD)		22.09	13.54
mean absolute deviation (MAD)		54.05	43.34
standard deviation (STD)		81.60	69.58

[a]In the bottom part, we present scaling factor and deviations obtained from the fitting of our data to the experimental ones.

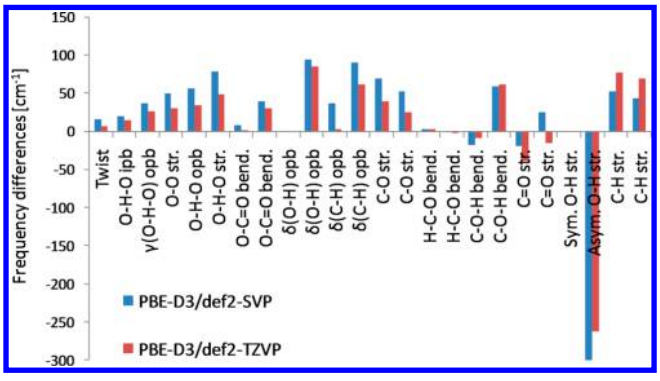


Figure 2. Differences between calculated (scaled) and experimental frequencies of the FAD in the gas phase.

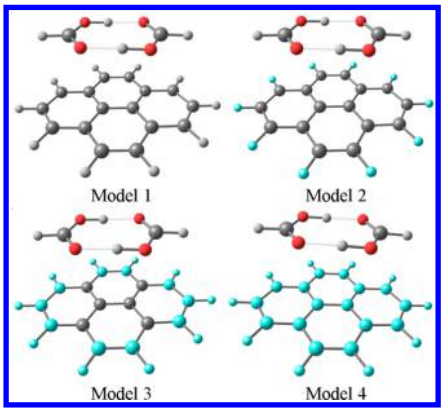


Figure 3. Model systems of FAD on pyrene. Model 1 without frozen atoms, Model 2 with frozen hydrogen atoms in pyrene, Model 3 with frozen hydrogens and outer carbons in pyrene, and Model 4 with frozen whole pyrene structure (H, light gray; C, dark gray; O, red; "frozen atoms", light blue).

carbon atoms only in the nanotube. To test the impact of this approximation, we tested in this work for the FAD−pyrene complex four approximations for the numerical calculation of the force constants for the internal vibrations of FAD, which are shown in Figure 3 and differ in the number of atoms in the pyrene subsystem that were kept frozen.

The comparison of the results from these four models is presented in Figure 4 and shows that freezing the vibrational modes of pyrene has a negligible effect on the spectroscopically interesting vibrational frequencies of the FAD. The deviations caused from freezing the nuclear motion of the pyrene subsystem are even smaller than those from the finite difference scheme, which is limited by the accuracy of the numerical integration of the exchange correlation functional.

This conclusion led us to use a numerical calculation for FAD inside SWCNT with all normal modes of the nanotube kept frozen so that only the force constants and vibrational frequencies for FAD were computed. Calculated frequency shifts are presented in Figure 5.

dx.doi.org/10.1021/jp411801h | J. Phys. Chem. C 2014, 118, 4483−4488

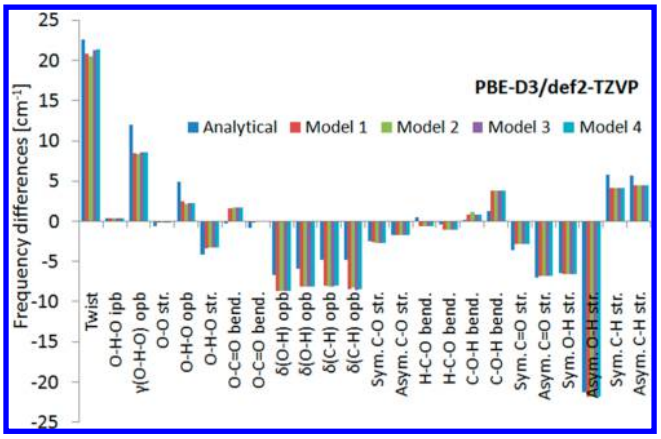


Figure 4. Changes of FAD vibrational frequencies between gas phase and on pyrene calculated analytically and numerically using models presented in Figure 3.

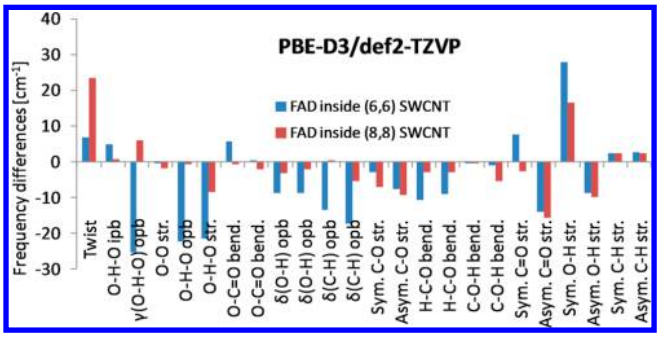


Figure 5. Changes of FAD vibrational frequencies between gas phase and inside carbon nanotubes calculated numerically with frozen SWCNT atoms.

The comparison of the vibrational frequencies of FAD in gas phase and inside the nanotubes reveals for most modes red shifts of the frequencies due to the confinement in the SWCNT. This tendency is especially observed for the out-of-plane bending of O−H and C−H groups and for the asymmetric C═O and O−H stretch modes. This can be an important indication for spectroscopists who will study such systems in the future. Similar as for the binding energy, we also observe for the vibrational spectrum that the interaction of FAD with the wider (8,8) SWCNT is considerably weaker than that with the smaller (6,6) SWCNT. Most frequency shifts are for the (8,8) SWCNT considerably smaller than for the (6,6) SWCNT. Exception are the asymmetric C═O and the low-frequency twist mode.

SUMMARY AND CONCLUSIONS

The results obtained in this study for the FAD−pyrene complex show a very good agreement of interaction energies obtained with DFT combined with the empirical D3 dispersion correction and spin-component scaled SCS-MP2. From this, one can conclude that DFT-D3 describes the interaction of organic acid dimers with large conjugated π-systems adequately and provides a good compromise between accuracy and computational costs in studies of very large molecular systems such as CNTs.

Our study shows that the interaction of the FAD with pyrene and two CNTs has only a negligible influence on the internal geometry of the FAD, although the interaction energy is, with 6−25 kcal/mol, sizable. The binding energy of FAD in SWCNT strongly depends on the radius of the nanotube and is larger the larger the contact surface is. Specifically, we find that the binding energy of FAD in the armchair (6,6) SWCNT is ca. 22 kcal/mol, whereas it is almost 25% smaller in the larger armchair (8,8) SWCNT.

Using a frozen atom approximation for the CNT, which was validated for the FAD−pyrene complex as model system and shown to introduce only negligible errors in the internal vibrational degrees of freedom of the FAD subsystem, allowed us the calculate vibrational frequencies for FAD inside the SWCNTs and to predict shifts of frequencies relative to the gas-phase values. The van der Waals interaction of the cyclic FAD with the SWCNTs has a small but visible impact on the vibrational frequencies of the FAD entity. We could, in particular, identify intense C−O, C═O, and O−H stretch modes as spectroscopic finger prints for the interaction of FAD with the CNTs, which could be used to detect such complexes in an experimental spectrum.

ASSOCIATED CONTENT

Supporting Information

Values of the HOMO−LUMO gaps as well as all calculated and scaled frequencies and the calculated IR intensities for studied FAD systems. This material is available free of charge via the Internet at http://pubs.acs.org.

AUTHOR INFORMATION

Corresponding Authors

*P.O.: E-mail: piotr.okrasinski@chem.uni.wroc.pl.
*Z.L.: E-mail: zdzislaw.latajka@chem.uni.wroc.pl.

Notes

The authors declare no competing financial interest.

ACKNOWLEDGMENTS

P.O. thanks RUB Computing Center for provision of computer time on Kopenhagen cluster.

REFERENCES

(1) Karousis, N.; Tagmatarchis, N.; Tasis, D. Current Progress on the Chemical Modification of Carbon Nanotubes. *Chem. Rev.* **2010**, *110*, 5366−5397.
(2) Albertorio, F.; Hughes, M. E.; Golovchenko, J. A.; Branton, D. Base Dependent DNA-Carbon Nanotube Interactions: Activation Enthalpies and Assembly-Disassembly Control. *Nanotechnology* **2009**, *20*, 395101.
(3) Foldvari, M.; Bagonluri, M. Carbon Nanotubes as Functional Excipients for Nanomedicines: II. Drug Delivery and Biocompatibility Issues. *Nanomedicine (N. Y., NY, U. S.)* **2008**, *4*, 183−200.
(4) Stepanian, S. G.; Karachevtsev, M. V.; Glamazda, A. Yu.; Karachevtsev, V. A.; Adamowicz, A. Stacking Interaction of Cytosine with Carbon Nanotubes: MP2, DFT and Raman Spectroscopy Study. *Chem. Phys. Lett.* **2008**, *459*, 153−158.
(5) Shukla, M. K.; Dubey, M.; Zakar, E.; Namburu, R.; Leszczynski, J. Density Functional Theory Investigation of Interaction of Zigzag (7,0) Single-walled Carbon Nanotube with Watson−Crick DNA Base Pairs. *Chem. Phys. Lett.* **2010**, *496*, 128−132.
(6) Pan, X.; Bao, X. The Effects of Confinement inside Carbon Nanotubes on Catalysis. *Acc. Chem. Res.* **2011**, *44*, 553−562.
(7) Wang, W.; Wang, D.; Zhang, Y.; Ji, B.; Tian, A. Hydrogen Bond and Halogen Bond inside the Carbon Nanotube. *J. Chem. Phys.* **2011**, *134*, 054317.
(8) Chang, K.; Kim, E.; Weck, P. F.; Tománek, D. Nanoconfinement Effects on the Reversibility of Hydrogen Storage in Ammonia Borane: A First-principles Study. *J. Chem. Phys.* **2011**, *134*, 214501.

(9) Kang, Y.; Liu, Y.-C.; Wang, Q.; Shen, J.-W.; Wu, T.; Guan, W.-J. On the Spontaneous Encapsulation of Proteins in Carbon Nanotubes. *Biomaterials* **2009**, *30*, 2807−2815.
(10) Chutia, A.; Hamada, I.; Tokuyama, M. Role of Lone Pair and π-orbital Interaction in Formation of Water Nanostructures Confined in Carbon Nanotubes. *Chem. Phys. Lett.* **2012**, *550*, 118−124.
(11) Alexiadis, A.; Kassinos, S. The Density of Water in Carbon Nanotubes. *Chem. Eng. Sci.* **2008**, *63*, 2047−2056.
(12) Zhu, F.; Schulten, K. Water and Proton Conduction through Carbon Nanotubes as Models for Biological Channels. *Biophys. J.* **2003**, *85*, 236−244.
(13) Hu, J.; Odom, T. W.; Lieber, C. M. Chemistry and Physics in One Dimension: Synthesis and Properties of Nanowires and Nanotubes. *Acc. Chem. Res.* **1999**, *32*, 435−445.
(14) Senthilkumar, L.; Ghanty, T. K.; Ghosh, S. K.; Kolandaivel, P. Hydrogen Bonding in Substituted Formic Acid Dimers. *J. Phys. Chem. A* **2006**, *110*, 12623−12628.
(15) Luckhaus, D. Hydrogen Exchange in Formic Acid Dimer: Tunnelling above the Barrier. *Phys. Chem. Chem. Phys.* **2010**, *12*, 8357−8361.
(16) Markwick, P. R. L.; Doltsinis, N. L.; Marx, D. Targeted Car−Parrinello Molecular Dynamics: Elucidating Double Proton Transfer in Formic Acid Dimer. *J. Chem. Phys.* **2005**, *122*, 054112.
(17) Smaga, A.; Sadlej, J. Computational Study on Interaction Energy Changes During Double Proton Transfer Process. *Comp. Theoretical Chem.* **2012**, *998*, 120−128.
(18) Thakkar, A. J. Small Clusters of Formic Acid: Tests and Applications of Density Functional Theory with Dispersion-correcting Potentials. *Chem. Phys. Lett.* **2013**, *560*, 71−74.
(19) Birer, Ö.; Havenith, M. High-resolution Infrared Spectroscopy of the Formic Acid Dimer. *Annu. Rev. Chem.* **2009**, *60*, 263−275.
(20) Ito, F. Infrared Spectra of $(HCOOH)_2$ and $(DCOOH)_2$ in Rare Gas Matrices: A Comparative Study with Gas Phase Spectra. *J. Chem. Phys.* **2008**, *128*, 114310.
(21) Zielke, P.; Suhm, M. A. Raman Jet Spectroscopy of Formic Acid Dimers: Low Frequency Vibrational Dynamics and Beyond. *Phys. Chem. Chem. Phys.* **2007**, *9*, 4528−4534.
(22) Durlak, P.; Latajka, Z. Car−Parrinello Molecular Dynamics and Density Functional Theory Simulations of Infrared Spectra for Acetic Acid Monomers and Cyclic Dimers. *Chem. Phys. Lett.* **2009**, *477*, 249−254.
(23) Durlak, P.; Berski, S.; Latajka, Z. Car-Parrinello and Path Integral Molecular Dynamics Study of the Hydrogen Bond in the Acetic Acid Dimer in the Gas Phase. *J. Mol. Model.* **2011**, *17*, 2995−3004.
(24) Ahlrichs, R.; Bär, M.; Häser, M.; Horn, H.; Kölmel, C. Electronic Structure Calculations on Workstation Computers: The Program System Turbomole. *Chem. Phys. Lett.* **1989**, *162*, 165−169.
(25) TURBOMOLE V6.4 2012, a development of University of Karlsruhe and Forschungszentrum Karlsruhe GmbH, 1989−2007, TURBOMOLE GmbH, since 2007; available from www.turbomole.com.
(26) Eichkorn, K.; Treutler, O.; Öhm, H.; Häser, M.; Ahlrichs, R. Auxiliary Basis Sets to Approximate Coulomb Potentials. *Chem. Phys. Lett.* **1995**, *242*, 652−660.
(27) Weigend, F.; Häser, M. RI-MP2: First Derivatives and Global Consistency. *Theor. Chem. Acc.* **1997**, *97*, 331−340.
(28) Weigend, F.; Häser, M.; Patzelt, H.; Ahlrichs, R. RI-MP2: Optimized Auxiliary Basis Sets and Demonstration of Efficiency. *Chem. Phys. Lett.* **1998**, *294*, 143−152.
(29) Bachorz, R. A.; Bischoff, F. A.; Glöβ, A.; Hättig, C.; Höfener, S.; Klopper, W.; Tew, D. P. The MP2-F12 Method in the TURBOMOLE Program Package. *J. Comput. Chem.* **2011**, *32*, 2492−2513.
(30) Eichkorn, K.; Weigend, F.; Treutler, O.; Ahlrichs, R. Auxiliary Basis Sets for Main Row Atoms and Transition Metals and Their Use to Approximate Coulomb Potentials. *Theor. Chem. Acc.* **1997**, *97*, 119−124.
(31) Weigend, F.; Köhn, A.; Hättig, C. Efficient Use of the Correlation Consistent Basis Sets in Resolution of the Identity MP2 Calculations. *J. Chem. Phys.* **2001**, *116*, 3175−3183.
(32) Hättig, C. Optimization of Auxiliary Basis Sets for RI-MP2 and RI-CC2 Calculations: Core-valence and Quintuple-ζ Basis Sets for H to Ar and QZVPP Basis Sets for Li to Kr. *Phys. Chem. Chem. Phys.* **2005**, *7*, 59−66.
(33) Schäfer, A.; Huber, C.; Ahlrichs, R. Fully Optimized Contracted Gaussian Basis Sets of Triple Zeta Valence Quality for Atoms Li to Kr. *J. Chem. Phys.* **1994**, *100*, 5829−5835.
(34) Schäfer, A.; Horn, H.; Ahlrichs, R. Fully Optimized Contracted Gaussian Basis Sets for Atoms Li to Kr. *J. Chem. Phys.* **1992**, *97*, 2571−2577.
(35) Kendall, R. A.; Dunning, T. H.; Harrison, R. J. Electron Affinities of the First-row Atoms Revisited. Systematic Basis Sets and Wave Functions. *J. Chem. Phys.* **1992**, *96*, 6796−6806.
(36) Peterson, K. A.; Adler, T. B.; Werner, H.-J. Systematically Convergent Basis Sets for Explicitly Correlated Wavefunctions: The Atoms H, He, B−Ne, and Al−Ar. *J. Chem. Phys.* **2008**, *128*, 084102.
(37) Boys, S. F.; Bernardi, F. The Calculation of Small Molecular Interactions by the Differences of Separate Total Energies. Some Procedures with Reduced Errors. *Mol. Phys.* **1970**, *19*, 553−566.
(38) Grimme, S.; Antony, J.; Ehrlich, S.; Krieg, H. A Consistent and Accurate Ab Initio Parametrization of Density Functional Dispersion Correction (DFT-D) for the 94 Elements H-Pu. *J. Chem. Phys.* **2010**, *132*, 154104.
(39) Grimme, S. Improved Second-order Møller−Plesset Perturbation Theory by Separate Scaling of Parallel- and Antiparallel-spin Pair Correlation Energies. *J. Chem. Phys.* **2003**, *118*, 9095−9102.
(40) Antony, J.; Grimme, S. Is Spin-Component Scaled Second-Order Møller−Plesset Perturbation Theory an Appropriate Method for the Study of Noncovalent Interactions in Molecules? *J. Chem. Phys. A* **2007**, *111*, 4862−4868.
(41) Hättig, C.; Klopper, W.; Köhn, A.; Tew, D. P. Explicitly Correlated Electrons in Molecules. *Chem. Rev.* **2012**, *112*, 4−74.
(42) Yousaf, K. E.; Peterson, K. A. Optimized Auxiliary Basis Sets for Explicitly Correlated Methods. *J. Chem. Phys.* **2008**, *129*, 184108.
(43) Helgaker, T.; Klopper, W.; Koch, H.; Noga, J. Basis-set Convergence of Correlated Calculations on Water. *J. Chem. Phys.* **1997**, *106*, 9639−9646.
(44) Almeningen, A.; Bastiansen, O.; Motzfeld, T. A Reinvestigation of the Structure of Monomer and Dimer Formic Acid by Gas Electron Diffraction Technique. *Acta Chem. Scand.* **1969**, *23*, 2848−2864.
(45) Weinhold, F. Nature of H-bonding in Clusters, Liquids, and Enzymes: An Ab Initio, Natural Bond Orbital Perspective. *J. Mol. Struct. THEOCHEM* **1997**, *398*−*399*, 181−197.
(46) Weinhold, F.; Landis, C. R. *Discovering Chemistry with Natural Bond Orbitals*; Wiley: Hoboken, NJ, 2012.
(47) Hill, J. G.; Platts, J. A.; Werner, H.-J. Calculation of Intermolecular Interactions in the Benzene Dimer Using Coupled-Cluster and Local Electron Correlation Methods. *Phys. Chem. Chem. Phys.* **2006**, *8*, 4072−4078.
(48) Grimme, S. On the Importance of Electron Correlation Effects for the π-π Interactions in Cyclophanes. *Chem.—Eur. J.* **2004**, *10*, 3423−3429.
(49) Piacenza, M.; Grimme, S. van der Waals Interactions in Aromatic Systems: Structure and Energetics of Dimers and Trimers of Pyridine. *ChemPhysChem* **2005**, *6*, 1554−1558.
(50) Nadykto, A. B.; Du, H.; Yu, F. Quantum DFT and DF-DFT Study of Sulfuric Acid, Sulfuric Acid Monohydrate, Formic Acid and Its Cyclic Dimer. *Vib. Spectrosc.* **2007**, *44*, 286−296.
(51) Latajka, Z.; Bouteiller, Y. Application of Density Functionals Methods for Study of Hydrogen-Bonded Systems: The Hydrogen Fluoride Dimer. *J. Chem. Phys.* **1994**, *101*, 9793−9799.